Journal of
Personalized Medicine

MDPI

Article

Baseline Biomarkers for Three-Year Fibrosis Development on OCT in Treatment-Naïve Neovascular AMD

Malcolm Fayers [1,*], Long T. Phan [2,3], Eden McDonogh [1], Kimberly L. Spooner [4,5,6], Andrew A. Chang [3,6,7], Hemal Mehta [3,6,7,8,9] and James G. Wong [3,6,7,8]

1 University of Sydney Medical School, Faculty of Medicine and Health, University of Sydney, Camperdown Campus, Sydney, NSW 2050, Australia
2 Cureos, Sydney, NSW 2000, Australia
3 Sydney Retina Clinic, Sydney, NSW 2000, Australia
4 NIHR Biomedical Research Centre, Moorfields Eye Hospital NHS Foundation Trust, UCL Institute of Ophthalmology, London EC1V 9EL, UK
5 Institute of Ophthalmology, University College London, London EC1V 9EL, UK
6 Save Sight Institute, University of Sydney, Sydney, NSW 2050, Australia
7 Strathfield Retina Clinic, Sydney, NSW 2135, Australia
8 Sydney Eye Hospital, Sydney, NSW 2000, Australia
9 School of Medicine, University of Notre Dame, Sydney Campus, Sydney, NSW 2007, Australia
* Correspondence: mal.fayers@gmail.com

Abstract

Aims: To explore how baseline biomarkers on optical coherence tomography (OCT) predict fibrotic development in eyes with neovascular age-related macular degeneration (nAMD) commencing intravitreal anti-vascular endothelial growth factor (anti-VEGF) therapy. **Methods:** Medical records at a single institution were retrospectively searched to identify eyes starting anti-vascular endothelial growth factor therapy with 36-month follow-up. Baseline OCT images were graded for central subfield thickness (CST) and nAMD lesion features. The development of fibrosis was determined after three years using an OCT-based approach, and multivariable logistic regression was used to identify independent predictors. **Results:** A total of 201 eyes were included, of mean age 77.3 years. At baseline, median visual acuity (VA) was 67 (IQR 58–77) letters, and mean central subfield thickness (CST) was 398.6 ± 135.3 µm. Mean injections received were 9.8 ± 1.9, 8.1 ± 3.1, and 7.3 ± 3.2 in years 1, 2, and 3, respectively. Fibrosis developed in 53 eyes (26.4%) by three years. Lower baseline VA (OR 0.68 per 10 letters, $p = 0.006$), as well as presence of subretinal hyperreflective material (SHRM; OR 10.80, $p < 0.001$), intraretinal fluid (IRF; OR 2.60, $p = 0.025$), and type 2 macular neovascularisation (MNV; OR 2.98, $p = 0.033$) were each independently associated with fibrosis, while drusen presence was protective (OR 0.25, $p = 0.002$). Fibrosis occurred in 4.6% of eyes without SHRM and 43.0% with SHRM. In exploratory unadjusted analyses, odds of fibrosis were higher with SHRM height 1–99 µm (OR 6.2, 95% CI 1.8–21.7) and ≥100 µm (OR 23.7, 95% CI 7.9–71.3) than with no SHRM, and higher with ≥100 µm than 1–99 µm (OR 3.8, 95% CI 1.6–9.1; $p = 0.003$). **Conclusions:** Subretinal hyperreflective material was the strongest baseline biomarker for developing subretinal fibrosis following anti-VEGF therapy in this historical cohort, with exploratory analyses suggesting higher risk at SHRM ≥ 100 µm. In combination with other biomarkers, these features may support future risk stratification in treatment-naïve neovascular age-related macular degeneration.

Keywords: neovascular age-related macular degeneration; subretinal fibrosis; subretinal hyperreflective material; optical coherence tomography; anti-VEGF therapy; risk stratification

Check for updates

Academic Editor: Livio Vitiello

Received: 29 September 2026
Revised: 19 October 2026
Accepted: 23 October 2026
Published: 30 October 2026

Copyright: © 2026 by the authors. Licensee MDPI, Basel, Switzerland. This article is an open access article distributed under the terms and conditions of the Creative Commons Attribution (CC BY) license.

1. Introduction

Anti-vascular endothelial growth factor (anti-VEGF) therapy has transformed the management of neovascular age-related macular degeneration (nAMD), substantially improving visual and anatomic outcomes over the past 15 years [1]. Despite these advances, fibrosis remains a common and sight-threatening complication, with a pooled incidence of approximately 29% across studies [2]. In the Comparison of Age-related Macular Degeneration Treatments Trials (CATT), fibrotic scar developed in 24.7% of eyes by two years, and scar of any type in 45.3%, with no association with drug or dosing regimen [3]. Fibrosis prevalence reaches 56% by five years [4]. Excessive fibrosis can result in irreversible damage to photoreceptors, retinal pigment epithelium (RPE) cells, and choroidal blood vessels, and is a major cause of severe visual loss in this disease [5].

The process is thought to arise from a maladaptive wound-healing response after choroidal neovascularisation, driven in part by the interplay between inflammation, angiogenesis, and endothelial–mesenchymal transition [6]. As such, the biological trigger of the so-called "angio-fibrotic switch", where pro-fibrotic pathways outweigh anti-angiogenic control, leading to the development of scar, remains poorly understood [5]. Consequently, there is currently no consensus regarding which imaging biomarkers reliably identify eyes at increased risk of fibrosis development following anti-VEGF therapy.

Several biomarkers, including subretinal hyperreflective material (SHRM), fibrovascular pigment epithelial detachment (fv-PED), and intraretinal fluid (IRF), have been associated with fibrosis development [4,7–10]. However, interpretation of the literature has been limited by inconsistent definitions of fibrosis, which have historically relied predominantly on colour fundus photography with variable incorporation of other modalities including optical coherence tomography (OCT) and fluorescein angiography (FA). Recently, the International Fibrosis Consensus (IFC) proposed a standardised spectral-domain optical coherence tomography (SD-OCT)-led framework for fibrosis detection [11]. The study aimed to determine whether baseline OCT biomarkers, graded using International Fibrosis Consensus-aligned criteria, predict fibrosis at three years in treatment-naïve nAMD.

2. Materials and Methods

2.1. Study Design and Participants

A single-centre retrospective audit was performed at Sydney Retina Clinic, Sydney, Australia, to identify consecutive patients who initiated treatment for the sole indication of nAMD between January 2009 and November 2017, using the clinic's pharmacy dispensing database and medical records. This study was performed in accordance with the Declaration of Helsinki. Ethical approval with a waiver of consent was provided by the Royal Australian and New Zealand College of Ophthalmologists ethics committee (#180.24).

Medical records of identified patients were manually examined to include patients who had SD-OCT (Spectralis OCT, Heidelberg Engineering GmbH, Heidelberg, Germany) performed at baseline, before the first anti-VEGF injection, and who had follow-up data for at least 36 months post initial injection. Patients were excluded if the study eye had a baseline visual acuity of worse than 35 Early Treatment of Diabetic Retinopathy Study (ETDRS) letters (equivalent to 20/200 on Snellen chart), if there was pre-existing fibrosis, if either eye had previously received any anti-VEGF treatment for any indication, if the study eye had previously been treated for neovascular age-related macular degeneration, including photodynamic therapy, or if they had participated in a clinical trial. Eyes were also excluded if there were co-existent ocular conditions likely to cause significant visual acuity loss during the observation period, or if any intervention during follow-up was expected to alter visual acuity substantially, such as YAG capsulotomy, cataract extraction, or vitrectomy. For patients who had a history of treatment involving both eyes, the eye first

treated was taken as the study eye. In those who initiated simultaneous anti-VEGF therapy in both eyes, the right eye was selected as the study eye.

2.2. Collection of Baseline and Outcome Variables

Patient characteristics (age, gender, and eye laterality) and treatment factors (initial anti-VEGF agent, the number of injections in each year after treatment initiation, and the number and timing of switches between anti-VEGF agents) were recorded from medical records. Anti-VEGF agents used were ranibizumab (Lucentis; Novartis, Basel, Switzerland), aflibercept 2 mg (Eylea; Bayer AG, Leverkusen, Germany) and bevacizumab (Avastin; Roche, Basel, Switzerland). Visual acuity was recorded clinically using Snellen charts and converted to approximate Early Treatment of Diabetic Retinopathy Study (ETDRS)-equivalent letter notation for analysis [12]. The 35-letter exclusion threshold was applied to these converted values rather than to acuity measured directly on an ETDRS chart.

Two graders independently examined OCT images (20° × 20°, 19-line raster) to classify baseline anatomic features. Any discrepancies were adjudicated by a senior medical retina specialist. Subretinal hyperreflective material (SHRM) was defined as hyperreflective tissue between the retinal pigment epithelium (RPE) and neurosensory retina; maximal SHRM height was also measured in µm (Figure 1). Pigment epithelial detachment (PED) was defined as any separation of the RPE to Bruch's membrane and was classified into a fibrovascular, serous, or drusenoid subtype, with drusenoid PED defined as ≥350 µm in width [13].

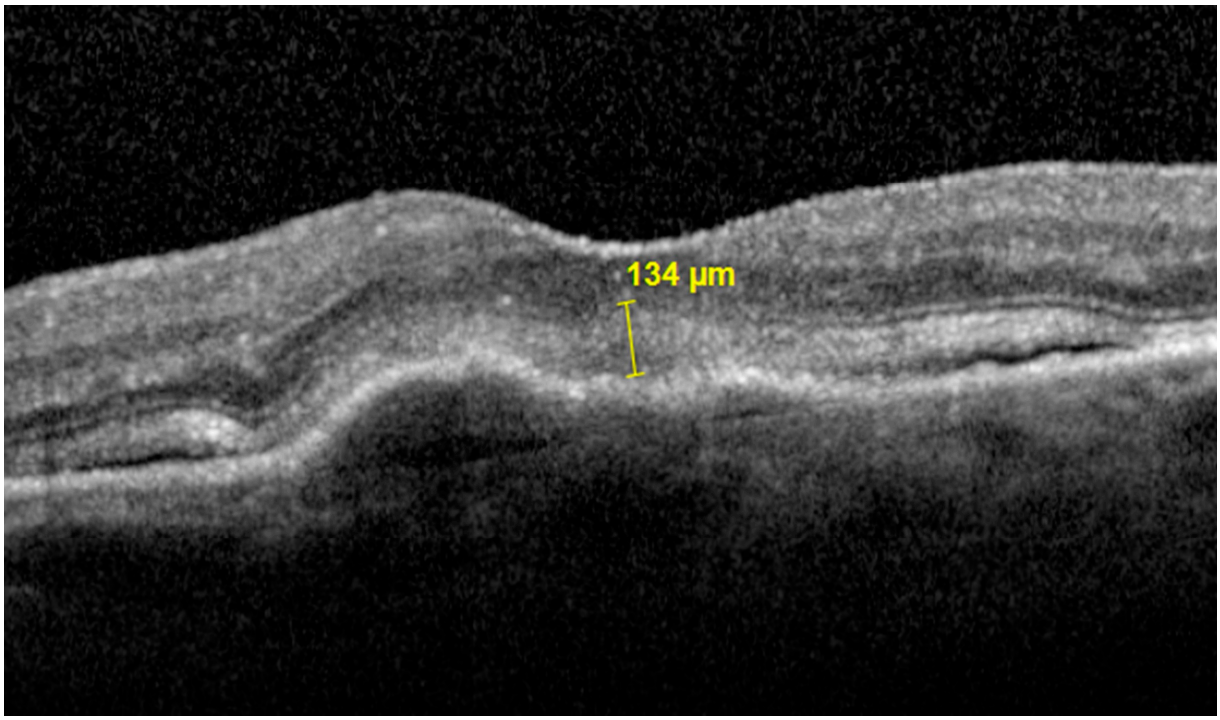


Figure 1. Maximum SHRM height measured manually with callipers on OCT.

The presence of drusen, subretinal drusenoid deposits (SDD), and macular atrophy (complete RPE and outer retinal atrophy (cRORA) ≥ 250 µm) [14] were also recorded. The presence of neovascular activity signs, intraretinal cystoid fluid (IRF), and subretinal fluid (SRF) were each recorded. Central-subfield thickness (CST) was measured as the average thickness between the ILM-BM within the central 1 mm diameter ETDRS subfield. Macular neovascularisation (MNV) lesion sub-type was classified using both OCT and FA at baseline.

2.3. Definition and Grading of Fibrosis

The development of fibrosis was assessed on the SD-OCT obtained at the visit nearest to three years (±3 months) after anti-VEGF initiation. Fibrosis was defined according to the International Fibrosis Consensus as highly hyperreflective material on SD-OCT with reflectivity greater than or equal to the RPE, well-defined margins, associated RPE disruption, and a laminated or band-like appearance [11]. Fibrosis was graded as present/absent using a two-step imaging approach. First, SD-OCT lesions were screened for the features described above. Secondly, these findings were corroborated using multicolour scanning laser ophthalmoscopy (SLO) imaging from the Spectralis platform or FA (Spectralis OCT, Heidelberg Engineering GmbH, Heidelberg, Germany), with near-infrared reflectance (NIR) used when other imaging modalities were unavailable (Figure 2). Grading of fibrosis at follow-up visits was performed prior to analysis of baseline images to mask graders against baseline features.

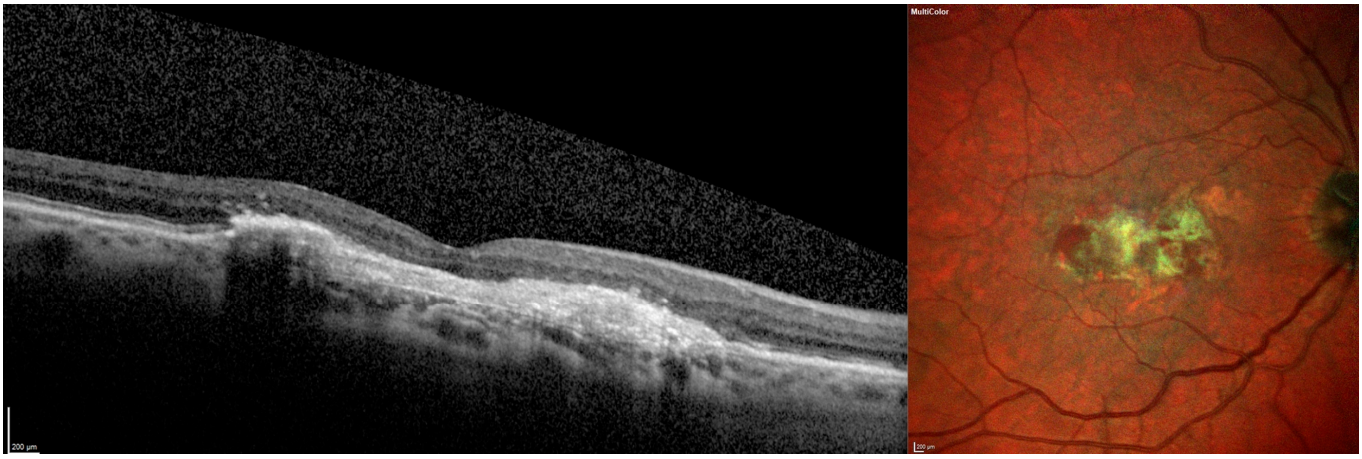


Figure 2. Detection of fibrosis on OCT using a two-step approach including OCT and multicolour SLO imaging.

2.4. Statistical Analysis

Baseline characteristics were summarised using descriptive statistics, with continuous variables reported as mean (standard deviation) or median (interquartile range) as appropriate, and categorical variables as frequency counts (percentage). Fibrosis development was reported as the cumulative incidence at three years (proportion of eyes). Associations between baseline variables (including treatment factors) with three-year fibrosis development were first explored using univariable logistic regression to identify candidate variables with $p < 0.05$, followed by multivariable logistic regression. CST was not entered due to collinearity with SHRM and to maintain approximately 10 events per variable. Complete-case analyses were performed throughout; no imputation was performed. The multivariable model included 197 eyes with complete covariate data (MNV type was missing in 4 eyes). All other baseline variables and the fibrosis outcome were complete. Model performance was assessed through the area under the curve (AUC) following receiver operating characteristic analysis. The effect of SHRM height was analysed separately as an exploratory, unadjusted analysis among subgroups (1–99 µm and ≥100 µm vs. no SHRM), and p values of less than 0.05 were considered statistically significant. Inter-rater agreement for fibrosis detection was assessed using percentage agreement and Cohen's kappa. IBM SPSS version 29 was used for all analyses (IBM Corporation, Armonk, NY, USA).

3. Results

A total of 409 eyes of 345 patients with treatment-naïve nAMD were identified. After inclusion of one eye per patient, 60 eyes were further excluded because of other retinal disease, prior treatment (e.g., laser photocoagulation) or participation in a clinical trial, and a further 84 eyes had less than 3 years of follow-up. This left a total of 201 eyes from 201 patients with treatment-naïve nAMD. Median follow-up interval was 36.1 months (IQR 35.6–36.5). Baseline characteristics are summarised in Table 1. There were 105 females (52.2%) with a mean age of 77.3 years (SD 8.5). The mean CST was 398.6 µm (SD 135.3). Median baseline VA was 67 letters (IQR 58–77). Type 1 macular neovascularisation was the commonest lesion subtype, present in 61.7% of eyes (124 of 201) at diagnosis. SHRM was present in 114 eyes (56.7%).

Table 1. Baseline characteristics of eyes.

Characteristic at Baseline	Eyes (n = 201)
Age, years, mean (SD)	77.25 (8.5)
Female, n (%)	105 (52.2)
Male, n (%)	96 (47.8)
Left eyes, n (%)	105 (52.2)
Right eyes, n (%)	96 (47.8)
VA at baseline, letters, median (IQR)	67.0 (58.0–77.0)
CST, mean µm (SD)	398.64 (135.3)
Anti-VEGF agent, n (%)	
Ranibizumab	103 (51.2)
Aflibercept	95 (47.3)
Bevacizumab	3 (1.5)
MNV subtype, n (%) **	
Type 1	124 (61.7)
Type 1—polypoidal	27 (13.4)
Type 2	29 (14.4)
Type 3	17 (8.5)
Drusen present, n (%)	92 (45.8)
Subretinal drusenoid deposits, n (%)	34 (16.9)
Macular atrophy, n (%)	20 (10.0)
Retinal fluid present, n (%)	190 (94.5)
Intraretinal fluid present, n (%)	101 (50.3)
Subretinal fluid present, n (%)	139 (69.2)
Pigment epithelial detachment present, n (%)	157 (78.1)
Subretinal hyperreflective material present, n (%)	114 (56.7)
SHRM height among eyes with SHRM (n = 114), mean µm (SD)	155.74 (100.0)

VA = visual acuity, CST = central subfield thickness, VEGF = vascular endothelial growth factor, MNV = macular neovascularisation. ** MNV subtype could not be assessed in 4 eyes because FA was unavailable or image quality was insufficient. Percentages are of 201 eyes.

Eyes received a mean of 9.8 ± 1.9 anti-VEGF injections in year 1, 8.1 ± 3.1 injections in year 2, and 7.3 ± 3.2 injections in year 3. Within the three-year follow-up, 57 eyes (28.4%)

switched anti-VEGF agents, of which two eyes (1.0%) switched twice. Most switching occurred from ranibizumab-treated eyes to aflibercept 2 mg ($n = 50$), with five aflibercept-treated eyes switching to ranibizumab, and two bevacizumab-treated eyes switching to aflibercept. First switches occurred in year 1 ($n = 17$), year 2 ($n = 18$), and year 3 ($n = 22$).

Fibrosis developed in 53 eyes (26.4%) by the end of follow-up at year 3. The overall percentage agreement for detection of fibrosis between two initial graders was 91%, with a Cohen's kappa score of 0.72 (0.53–0.88). Univariable and multivariable logistic regression analyses for predictors of fibrosis at three years are shown in Table 2. In univariable analysis, baseline SHRM was associated with substantially higher odds of fibrosis at three years (OR 15.64, 95% CI 5.37–45.59; $p < 0.001$). Drusen presence was inversely associated with fibrosis (OR 0.22, 95% CI 0.10–0.45; $p < 0.001$). IRF was associated with increased odds of fibrosis (OR 2.42, 95% CI 1.26–4.65; $p = 0.008$), while SRF was not (OR 1.74, 95% CI 0.84–3.61; $p = 0.135$). Poorer baseline VA (OR 0.59 per 10 letters, 95% CI 0.47–0.75; $p < 0.001$) and thicker CST (OR 1.91 per 100 µm, 95% CI 1.42–2.59; $p < 0.001$) were both associated with fibrosis, as was MNV type 2 compared with type 1 (OR 5.34, 95% CI 2.27–12.57; $p < 0.001$). Age, gender, PED subtype, SDD, and the number of injections in year 1 were not significantly associated with fibrosis.

Table 2. Baseline OCT biomarkers associated with three-year fibrosis.

	Univariable		Multivariable	
Variable	***p* Value**	**OR (95% CI)**	***p* Value**	**OR (95% CI)**
Age (per year)	0.128	1.03 (0.99–1.07)	-	-
Gender (male vs. female)	0.135	1.62 (0.86–3.05)	-	-
VA (per 10 ETDRS letters)	<0.001	0.59 (0.47–0.75)	0.006	0.68 (0.52–0.90)
CST (per 100 µm) *	<0.001	1.91 (1.42–2.59)	-	-
MNV type (vs. type 1)				
Type 2 **	<0.001	5.34 (2.27–12.57)	0.033	2.98 (1.09–8.12)
Type 3	0.809	1.16 (0.35–3.86)	-	-
PCV ***	0.775	0.86 (0.30–2.48)	-	-
SHRM (present vs. absent)	<0.001	15.64 (5.37–45.59)	<0.001	10.80 (3.47–33.59)
IRF (present vs. absent)	0.008	2.42 (1.26–4.65)	0.025	2.60 (1.13–5.98)
SRF (present vs. absent)	0.135	1.74 (0.84–3.61)	-	-
PED type (vs. no PED)				
Fibrovascular	0.354	1.46 (0.65–3.27)	-	-
Serous	0.837	0.89 (0.28–2.78)	-	-
Drusenoid	0.358	0.30 (<0.01–3.01)	-	-
Drusen (present vs. absent)	<0.001	0.22 (0.10–0.45)	0.002	0.25 (0.10–0.61)
SDD (present vs. absent)	0.403	0.68 (0.28–1.67)	-	-
Injections in year 1 (per injection)	0.146	1.13 (0.96–1.34)	-	-

Univariable analyses included $n = 201$, except MNV type $n = 197$. The multivariable model included 197 eyes (52 fibrosis events) with complete covariate data (MNV type was missing in 4 eyes). * CST was excluded from the multivariable model owing to collinearity with SHRM and the limited number of events, and to allow for an events-per-variable ratio of 10. ** In the multivariable model, MNV type 2 was compared against all other MNV types (1, 3, and PCV combined). *** PCV = polypoidal choroidal vasculopathy.

In multivariable analysis, poorer baseline VA (adjusted OR 0.68 per 10 letters, 95% CI 0.52–0.90; $p = 0.006$), MNV type 2 (adjusted OR 2.98, 95% CI 1.09–8.12; $p = 0.033$), SHRM (adjusted OR 10.80, 95% CI 3.47–33.59; $p < 0.001$), and IRF (adjusted OR 2.60, 95% CI 1.13–5.98; $p = 0.025$) remained independently associated with fibrosis at three years. Drusen presence remained protective (adjusted OR 0.25, 95% CI 0.10–0.61; $p = 0.002$). The model showed good discrimination, with an apparent AUC of 0.872 (95% CI 0.812–0.925) (Figure 3).

In exploratory, stratified analyses by maximum SHRM height, three-year fibrosis event rate was 4/87 (4.6%) among eyes without any SHRM at baseline, 9/39 (23.1%) among eyes with SHRM 1–99 µm, and 40/75 (53.3%) among eyes with SHRM height ≥ 100 µm at baseline (Figure 4). Odds of developing fibrosis significantly increased for both SHRM height 1–99 µm (unadjusted OR 6.2, 95% CI 1.8–21.7, $p = 0.004$) and ≥100 µm (unadjusted OR 23.7, 95% CI

7.9–71.3, $p < 0.001$) compared to no SHRM. Among SHRM groups, the odds of developing fibrosis were significantly greater among eyes with SHRM height ≥ 100 µm vs. 1–99 µm at baseline (unadjusted OR 3.8, 95% CI 1.6–9.1, $p = 0.003$).

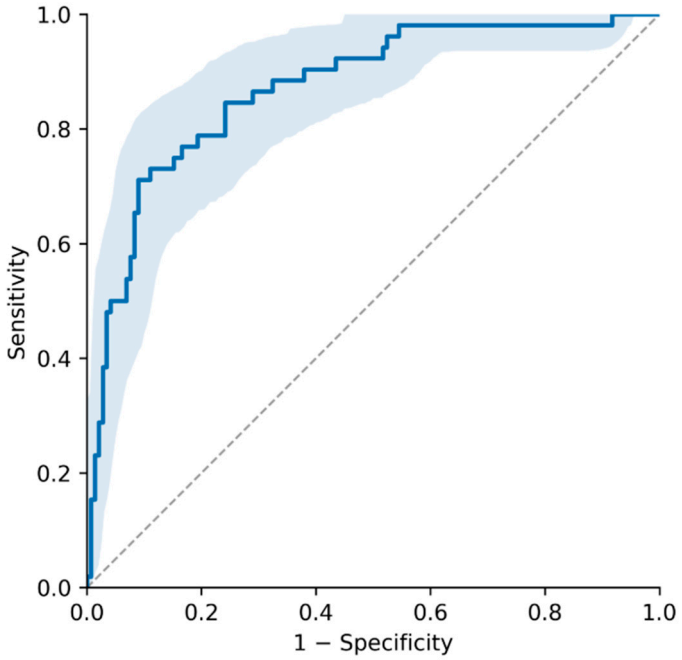


Figure 3. Multivariable ROC curve for three-year fibrosis prediction. The solid blue line is the ROC curve of the multivariable model (apparent AUC 0.87, 95% CI 0.81–0.93), the shaded blue area is the 95% confidence band around the curve, and the dashed grey diagonal indicates no discrimination (AUC 0.5).

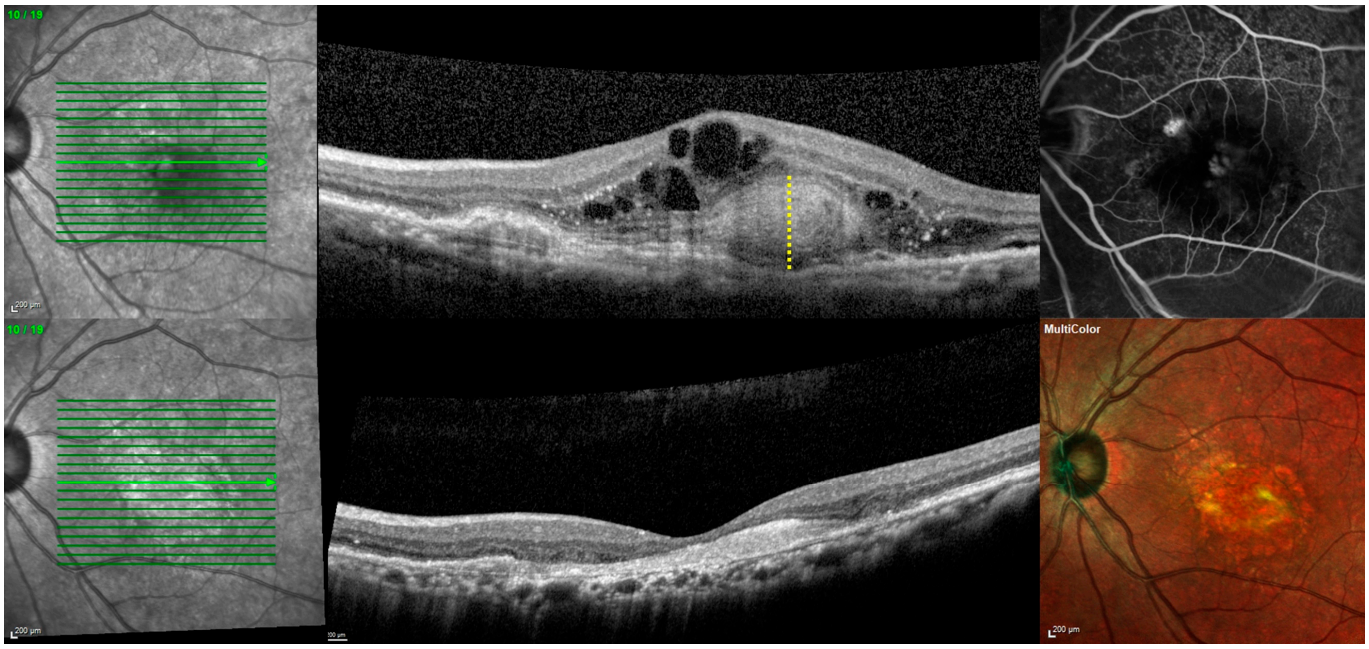


Figure 4. Example of baseline SHRM and subsequent fibrosis in the same eye. **Upper row**, baseline: NIR 19-line raster scan pattern (green lines; the line with the arrowhead marks the B-scan displayed), SD-OCT B-scan showing SHRM with maximum height measured between the dotted yellow line, and fluorescein angiogram. **Lower row**, three years later: NIR image with the raster pattern, SD-OCT B-scan showing fibrosis, and multicolor SLO image.

4. Discussion

Subretinal fibrosis is one of the final complications of nAMD that causes irreversible vision loss and remains a diagnostic and therapeutic challenge. Using a recently proposed OCT-based approach for fibrosis identification, this study found a fibrosis incidence of 26.4% after initiating anti-VEGF therapy, a rate comparable to pooled cumulative incidence rates in prior studies at 29% [2]. This likely reflects both the OCT-led fibrosis definition used here and a proactive tapering injection pattern consistent with treat-and-extend dosing, which is linked to the lowest pooled fibrosis rates [2]. This study found that SHRM presence, IRF presence, type 2 MNV, lower baseline VA, and drusen absence were each independently associated with fibrosis development after three years of anti-VEGF therapy. Among these, SHRM at baseline was the strongest predictor, and exploratory analyses suggested higher odds of fibrosis with SHRM height ≥ 100 µm than with 1–99 µm.

SHRM is widely considered an OCT-based precursor to the development of fibrosis, but not all SHRM progresses to fibrosis. SHRM itself represents a multitude of components, including MNV, blood, fibrin, inflammatory, and vitelliform material [9]. While many of these are associated with fibrosis, studies report that undefined hyperreflective material, such as that which does not meet the OCT definitions of SHRM, has the capacity to resolve [7]. On the other hand, multiple studies have now shown a relationship between the presence of SHRM and the development of fibrosis [2,7,15].

A recent systematic review and meta-analysis reported pooled odds ratios of 2.7 (95% CI 1.1–6.6) for baseline SHRM and 5.7 for type 2 MNV [2]. Our adjusted type 2 MNV association (OR 2.98, 95% CI 1.09–8.12, compared with all other lesion types) was smaller than the pooled estimate. In contrast, our SHRM association (OR 10.80, 95% CI 3.47–33.59) was considerably larger than the pooled estimate [2]. This may be explained by our OCT-anchored SHRM definition, treatment-naïve baseline population avoiding SHRM impact through anti-VEGF exposure, and three-year treatment window compared to the shorter follow-up period of the pooled studies. By measuring height, our study extends these findings by quantifying SHRM height, suggesting a higher fibrosis risk at SHRM height ≥ 100 µm. In the CATT, scar at two years was more frequent in eyes with persistent SHRM than in eyes in which SHRM resolved (64% vs. 31%) [15]. Additionally, animal laser models show that myofibroblast-rich early subretinal granulation tissue, which may form more well defined SHRM, expands and then scars [16,17], which may help explain our findings. As nAMD progresses and the angio-fibrotic switch occurs, macrophage infiltration, pericyte to myofibroblast transition, and persistent transforming growth factor beta (TGF-β) signalling predominate, leading to the formation of scar [18]. Our findings are compatible with the possibility that this switch is more likely to occur at ≥100 µm of SHRM height, though this was not formally tested and does not establish causality.

Baseline IRF was independently associated with fibrosis (adjusted OR 2.6, 95% CI 1.1–6.0), consistent with the pooled estimate of a recent meta-analysis (OR 3.6, 95% CI 0.9–14.8) [2]. Previous analyses show IRF as associated with poorer visual outcomes and progression of nAMD, particularly when involving the fovea [19]. Unlike SHRM, which is an OCT precursor of fibrotic tissue, IRF is more likely to represent disease severity and is associated with worse visual outcomes [10]. IRF may therefore cluster with other severity indicators in univariable analysis. Further studies with time-updated fluid measures are required to separate the prognostic contribution of IRF from that of overall disease severity. Conversely, our SRF OR of 1.74 (0.84–3.61) points the opposite way to the pooled estimate of 0.61 (0.27–1.36), though both cross-unity and heterogeneity there was extreme (I^2 = 97%). The proposed explanation in that review is lesion-type confounding—SRF is commoner in type 1 MNV, which is itself lower-risk—so our result may reflect a different lesion mix [2].

The protective role of drusen has more recently been postulated as part of a lesion compartment theory, whereby both drusen and subretinal drusenoid deposits are separate pathological entities occurring in different parts of the retina. Large soft drusen and basal laminar deposits thicken the Bruch's membrane-RPE complex, thus favouring type 1 neovascularisation, which rarely breaches the external limiting membrane [20]. Type 3 MNV, by contrast, is retinal in origin, arising from the deep capillary plexus and growing outward towards the outer retina [21]. These phenotypes have a predisposition towards atrophy rather than scar [21]. Conversely, eyes with little or no drusen often develop type 2 choroidal neovascularisation, which grows directly into the subretinal space and appears to be highly fibrogenic [5]. It may be that this AMD phenotype has an inclination towards fibroplasia rather than RPE atrophy. Like IRF, the absence of drusen may be an imaging surrogate for disease activity, which may explain its association with other univariable regression factors such as VA. This study quantifies the risk reduction in the presence of drusen, providing a counterbalance for the risk created by greater SHRM height.

In terms of injection frequency, pooled literature shows that the incidence of fibrosis is substantially lower under treat-and-extend dosing (24.2%, 95% CI 15.8–35.1) than under monthly (40.0%, 95% CI 39.9–40.1) or pro re nata regimens (46.6%, 95% CI 45.0–48.2), implying that more proactive treatment may reduce fibrosis risk overall rather than increasing it [2]. Our results did not find associations for injection frequency in the first year, though this may have been limited by the lack of variability in treatment frequency amongst eyes in the first year of treatment, as all eyes were managed under a similar treat-and-extend regimen with a loading dose. Injection patterns and treatment switches after baseline may be a consequence rather than a cause of fibrosis, as treatment may be extended, reduced, or discontinued once scarring develops. Because the date of first fibrosis detection was not captured, the temporal relationship between these post-baseline treatment factors and fibrosis could not be established, so they were not included in the baseline model, and actual injection intervals were not analysed. Year-1 injection number does not fully characterise treatment exposure, so residual confounding by treatment pattern is possible.

The strengths of this study include its longitudinal assessment of a treatment-naïve cohort using one eye per patient, with patients identified at initiation of anti-VEGF therapy. The use of a pharmacy dispensing database to identify patients allowed for consecutive identification at treatment initiation, and the three-year follow-up enabled assessment of fibrosis at a clinically relevant point in time. An additional strength was the independent grading of fibrosis, using a consensus-aligned outcome definition. Inter-rater agreement in fibrosis detection using this approach was high ($k = 0.72$), exceeding that reported in previous studies ($k = 0.4$–0.6) [2].

In terms of limitations, an important consideration was that although our protocol was consensus aligned, it did not explicitly follow the two-step IFC pathway, as NIR was substituted for multicolour SLO imaging or FA when these modalities were unavailable. Furthermore, images were obtained from real-world practice and were not subject to the same quality standards as clinical trials. This may have reduced the sensitivity of fibrosis detection and resulted in underestimation of its incidence. We were also unable to capture baseline subretinal haemorrhage ≥4 disc diameters, an established predictor of fibrosis (pooled OR 2.3, 95% CI 1.2–4.2) [2], which represents a source of residual confounding not accounted for in our model. Within the association between fibrosis risk and SHRM height, wide confidence intervals and few events in the subgroups limit the precision of the stratified estimates. The multivariable model was based on 52 events, which limited the number of covariates, and its discrimination (apparent AUC 0.872) has not been validated internally or externally. In addition, anatomical instability over the 36-month follow-up period, particularly CST fluctuation, has similarly been linked to incident fibrosis in prior work [22,23]

and was not captured here, representing a further avenue for residual confounding and a target for future analysis.

Our cohort was drawn from historical records before the use of faricimab (Roche, Basel, Switzerland) or aflibercept 8 mg (Bayer AG, Leverkusen, Germany) as first-line agents and more recent treat-and-extend recommendations [24]. These newer agents aim to allow disease control at longer treatment intervals, and CST fluctuation has been linked to fibrosis [23], so contemporary fibrosis rates may differ from those we report. The baseline predictors may still apply given they describe treatment-naïve eyes, but absolute incidence under current regimens may differ, and although modern practice will often tolerate some SRF [25], IRF remains a biomarker that is generally treated as a marker of disease activity [19,26]. The study was also retrospective, single-centre, and used Snellen-derived VA rather than true ETDRS.

Additionally, restricting the analysis to eyes with three years of follow-up may have introduced attrition or survivorship bias. Of the eligible eyes identified, 84 (29.5%) did not complete three years of follow-up, a proportion comparable to that reported in other real-world nAMD cohorts [27]. No baseline or follow-up data was collected for these patients, so we could not compare them or perform a sensitivity analysis. Loss to follow-up has been associated with several factors including older age, treatment costs, poorer baseline visual acuity, and poor early response to treatment [27]. Since poorer baseline visual acuity was itself associated with fibrosis in our cohort, the incidence of fibrosis may have been underestimated, and the effect on the odds ratios is uncertain.

This study supports the literature that SHRM presence is associated with disease progression and adds a quantitative element to imaging. Future multi-centre studies can provide more detailed multivariable analysis, validation, and an increase in the number of biomarkers by expanding the study numbers across multiple populations. Incorporating an artificial intelligence (AI) volumetric analysis of SHRM could allow further exploration of the association between SHRM severity and fibrosis development. Combined, this could lead to the development of a baseline fibrosis risk stratification algorithm that can calculate risk in real time for treatment-naïve patients, though this would require external validation. Finally, further work identifying compartment-specific outcomes is needed given the differences in lesion phenotype based on location.

5. Conclusions

Overall, SHRM presence and drusen status on baseline OCT were independently associated with three-year fibrosis in this historical cohort of treatment-naïve nAMD and may help identify eyes at higher risk. Exploratory analyses suggested higher odds of fibrosis with SHRM height ≥ 100 µm than with 1–99 µm. Eyes with SHRM at baseline may therefore warrant closer monitoring for progression to fibrosis, and this information may help inform prognostic counselling at treatment initiation. These findings require prospective, externally validated assessment before they can inform treatment regimens in practice.

Author Contributions: Conceptualisation, M.F., L.T.P., J.G.W. and H.M. Methodology, L.T.P. and J.G.W. Software, M.F. and L.T.P. Validation, M.F., L.T.P. and K.L.S. Formal analysis, M.F., L.T.P. and K.L.S. Resources, J.G.W., H.M., and A.A.C. Writing—original draft preparation, M.F. and E.M. Writing—review and editing, L.T.P., J.G.W., E.M., K.L.S. and H.M. Supervision, J.G.W. All authors have read and agreed to the published version of the manuscript.

Funding: This research received no external funding.

Institutional Review Board Statement: This study was performed in accordance with the Declaration of Helsinki. Ethical approval with a waiver of consent was provided by the Human Research Ethics Committee of the Royal Australian and New Zealand College of Ophthalmologists (RANZCO)

(HREC #180.24) approved 21 August 2024. The study was conducted at Sydney Retina Clinic, Sydney, Australia.

Informed Consent Statement: Patient consent was waived by the ethics committee because this was a retrospective audit of clinical records and imaging obtained as part of routine care, with no patient contact, intervention or change to treatment, so involvement carried very low risk. Obtaining consent was impracticable: the cohort comprised 345 patients treated between 2009 and 2017 with a mean age of 77.3, many of whom had stopped attending the clinic, had moved, or were likely to be deceased or unable to give consent, and contacting them would have required identifying patients and re-accessing their records beyond the purpose of the audit. There was no known or likely reason to believe that patients would have objected to the use of their routine clinical data for this purpose. Privacy and confidentiality were protected by de-identifying the data for analysis and storing it on secure, access-restricted clinic systems.

Data Availability Statement: Supportive data was used from a single centre and is not publicly available. The data comes from a retrospective audit of patient records with consent waived under ethics approval. The corresponding author can share de-identified data on reasonable request, provided the ethics committee and the institutions involved approve.

Conflicts of Interest: H.M. has been involved as a consultant for 4DMT, AbbVie, Alcon, Apellis, Astellas, Bayer, Boehringer Ingelheim, Filamon, Heidelberg Engineering, Optigo Biotherapeutics, Ripple Therapeutics and Roche. J.W. has been a study investigator, consultant, and advisory board member for Apellis, Bayer, Regeneron, Exonate, Novartis, Ocular Therapeutix, Ripple Therapeutics, Roche/Genentech, Alexion, Janssen/Johnson & Johnson, Kyowa Kirin, EyeBio, Belite Bio. A.C. has consulted for Novartis, Bayer, Roche, Opthea, Apellis, Astellas, Zeissand Alcon. L.T.P. is employed by Cureos, an independent research centre. Cureos had no commercial involvement in the study and no role in its design, execution, interpretation, or writing. The remaining authors declare no conflicts of interest.

References

1. Finger, R.P.; Daien, V.; Eldem, B.M.; Talks, J.S.; Korobelnik, J.-F.; Mitchell, P.; Sakamoto, T.; Wong, T.Y.; Pantiri, K.; Carrasco, J. Anti-vascular endothelial growth factor in neovascular age-related macular degeneration—A systematic review of the impact of anti-VEGF on patient outcomes and healthcare systems. *BMC Ophthalmol.* **2020**, *20*, 294. [CrossRef] [PubMed]
2. Spooner, K.L.; Fraser-Bell, S.; Fu, D.J.; Faes, L.; Romano, F.; Cozzi, M.; Chang, A.A.; Sivaprasad, S. Imaging and functional correlates of fibrosis in neovascular age-related macular degeneration: A systematic review. *Front. Ophthalmol.* **2026**, *6*, 1786309. [CrossRef] [PubMed]
3. Daniel, E.; Toth, C.A.; Grunwald, J.E.; Jaffe, G.J.; Martin, D.F.; Fine, S.L.; Huang, J.; Ying, G.S.; Hagstrom, S.A.; Winter, K.; et al. Risk of scar in the comparison of age-related macular degeneration treatments trials. *Ophthalmology* **2014**, *121*, 656–666. [CrossRef] [PubMed]
4. Cheong, K.X.; Cheung, C.M.G.; Teo, K.Y.C. Review of Fibrosis in Neovascular Age-Related Macular Degeneration. *Am. J. Ophthalmol.* **2023**, *246*, 192–222. [CrossRef] [PubMed]
5. Tenbrock, L.; Wolf, J.; Boneva, S.; Schlecht, A.; Agostini, H.; Wieghofer, P.; Schlunck, G.; Lange, C. Subretinal fibrosis in neovascular age-related macular degeneration: Current concepts, therapeutic avenues, and future perspectives. *Cell Tissue Res.* **2022**, *387*, 361–375. [CrossRef] [PubMed]
6. McLellan, F.C.; Huang, K.; Wong, E.; Shu, D.Y. The Angiofibrotic Switch in Retinal and Choroidal Vascular Diseases: Mechanistic Drivers of Angiogenesis and Endothelial-Mesenchymal Transition. *Am. J. Pathol.* **2025**, *195*, 1363. [PubMed]
7. Casalino, G.; Stevenson, M.R.; Bandello, F.; Chakravarthy, U. Tomographic Biomarkers Predicting Progression to Fibrosis in Treated Neovascular Age-Related Macular Degeneration: A Multimodal Imaging Study. *Ophthalmol. Retin.* **2018**, *2*, 451–461. [CrossRef] [PubMed]
8. Olivieri, C.; Perin, G.; Zhuang, X.; Neri, G.; Parisi, G.; Marolo, P.; Viggiano, P.; Boscia, F.; Reibaldi, M.; Borrelli, E. Baseline Optical Coherence Tomography Biomarkers Associated with the 2-Year Development of Macular Atrophy or Fibrosis in Neovascular Age-related Macular Degeneration. *Ophthalmol. Sci.* **2026**, *6*, 101268. [PubMed]
9. Bachmeier, I.; Armendariz, B.G.; Yu, S.; Jäger, R.J.; Ebneter, A.; Glittenberg, C.; Pauleikhoff, D.; Sadda, S.R.; Chakravarthy, U.; Fauser, S. Fibrosis in neovascular age-related macular degeneration: A review of definitions based on clinical imaging. *Surv. Ophthalmol.* **2023**, *68*, 835–848. [CrossRef] [PubMed]
10. Hanson, R.L.W.; Airody, A.; Sivaprasad, S.; Gale, R.P. Optical coherence tomography imaging biomarkers associated with neovascular age-related macular degeneration: A systematic review. *Eye* **2023**, *37*, 2438–2453. [CrossRef] [PubMed]

11. Chakravarthy, U.; Csincsik, L.; Teo, K.Y.C.; Munk, M.R.; Grewal, D.S.; Guymer, R.H.; Jaffe, G.J.; Peto, T.; Sadda, S.R.; Staurenghi, G.; et al. Standardization of Imaging Criteria for Detecting Macular Fibrosis in Neovascular Age-Related Macular Degeneration. *Ophthalmol. Sci.* **2026**, *6*, 101027. [CrossRef] [PubMed]
12. Gregori, N.Z.; Feuer, W.; Rosenfeld, P.J. Novel method for analyzing snellen visual acuity measurements. *Retina* **2010**, *30*, 1046. [CrossRef] [PubMed]
13. Spaide, R.F.; Jaffe, G.J.; Sarraf, D.; Freund, K.B.; Sadda, S.R.; Staurenghi, G.; Waheed, N.K.; Chakravarthy, U.; Rosenfeld, P.J.; Holz, F.G.; et al. Consensus Nomenclature for Reporting Neovascular Age-Related Macular Degeneration Data: Consensus on Neovascular Age-Related Macular Degeneration Nomenclature Study Group. *Ophthalmology* **2020**, *127*, 616–636. [CrossRef] [PubMed]
14. Sadda, S.R.; Guymer, R.; Holz, F.G.; Schmitz-Valckenberg, S.; Curcio, C.A.; Bird, A.C.; Blodi, B.A.; Bottoni, F.; Chakravarthy, U.; Chew, E.Y.; et al. Consensus Definition for Atrophy Associated with Age-Related Macular Degeneration on OCT: Classification of Atrophy Report 3. *Ophthalmology* **2018**, *125*, 537–548. [PubMed]
15. Willoughby, A.S.; Ying, G.S.; Toth, C.A.; Maguire, M.G.; Burns, R.E.; Grunwald, J.E.; Daniel, E.; Jaffe, G.J. Subretinal Hyperreflective Material in the Comparison of Age-Related Macular Degeneration Treatments Trials. *Ophthalmology* **2015**, *122*, 1846–1853.e1845. [CrossRef] [PubMed]
16. Grossniklaus, H.E.; Kang, S.J.; Berglin, L. Animal models of choroidal and retinal neovascularization. *Prog. Retin. Eye Res.* **2010**, *29*, 500–519. [CrossRef] [PubMed]
17. Little, K.; Llorián-Salvador, M.; Tang, M.; Du, X.; Marry, S.; Chen, M.; Xu, H. Macrophage to myofibroblast transition contributes to subretinal fibrosis secondary to neovascular age-related macular degeneration. *J. Neuroinflamm.* **2020**, *17*, 355. [CrossRef] [PubMed]
18. Higashijima, F.; Hasegawa, M.; Yoshimoto, T.; Kobayashi, Y.; Wakuta, M.; Kimura, K. Molecular mechanisms of TGFβ-mediated EMT of retinal pigment epithelium in subretinal fibrosis of age-related macular degeneration. *Front. Ophthalmol.* **2023**, *2*, 1060087. [CrossRef] [PubMed]
19. Kodjikian, L.; Parravano, M.; Clemens, A.; Dolz-Marco, R.; Holz, F.G.; Munk, M.R.; Nicolò, M.; Ricci, F.; Silva, R.; Talks, S.J.; et al. Fluid as a critical biomarker in neovascular age-related macular degeneration management: Literature review and consensus recommendations. *Eye* **2021**, *35*, 2119–2135. [CrossRef] [PubMed]
20. Sura, A.A.; Chen, L.; Messinger, J.D.; Swain, T.A.; McGwin, G., Jr.; Freund, K.B.; Curcio, C.A. Measuring the Contributions of Basal Laminar Deposit and Bruch's Membrane in Age-Related Macular Degeneration. *Investig. Ophthalmol. Vis. Sci.* **2020**, *61*, 19. [CrossRef] [PubMed]
21. Clemens, C.R.; Eter, N.; Alten, F. Current Perspectives on Type 3 Macular Neovascularization due to Age-Related Macular Degeneration. *Ophthalmologica* **2024**, *247*, 73–84. [CrossRef] [PubMed]
22. Romano, F.; Cozzi, E.; Airaldi, M.; Nassisi, M.; Viola, F.; Aretti, A.; Milella, P.; Giuffrida, F.P.; Teo, K.C.Y.; Cheung, C.M.G.; et al. Ten-Year Incidence of Fibrosis and Risk Factors for Its Development in Neovascular Age-Related Macular Degeneration. *Am. J. Ophthalmol.* **2023**, *252*, 170–181. [CrossRef] [PubMed]
23. Evans, R.N.; Reeves, B.C.; Maguire, M.G.; Martin, D.F.; Muldrew, A.; Peto, T.; Rogers, C.; Chakravarthy, U. Associations of Variation in Retinal Thickness with Visual Acuity and Anatomic Outcomes in Eyes with Neovascular Age-Related Macular Degeneration Lesions Treated with Anti-Vascular Endothelial Growth Factor Agents. *JAMA Ophthalmol.* **2020**, *138*, 1043–1051. [CrossRef] [PubMed]
24. Chaikitmongkol, V.; Sagong, M.; Lai, T.Y.Y.; Tan, G.S.W.; Ngah, N.F.; Ohji, M.; Mitchell, P.; Yang, C.-H.; Ruamviboonsuk, P.; Wong, I.; et al. Treat-and-Extend Regimens for the Management of Neovascular Age-related Macular Degeneration and Polypoidal Choroidal Vasculopathy: Consensus and Recommendations from the Asia-Pacific Vitreo-retina Society. *Asia Pac. J. Ophthalmol.* **2021**, *10*, 507–518. [CrossRef] [PubMed]
25. Guymer, R.H.; Markey, C.M.; McAllister, I.L.; Gillies, M.C.; Hunyor, A.P.; Arnold, J.J. Tolerating Subretinal Fluid in Neovascular Age-Related Macular Degeneration Treated with Ranibizumab Using a Treat-and-Extend Regimen: FLUID Study 24-Month Results. *Ophthalmology* **2019**, *126*, 723–734. [CrossRef] [PubMed]
26. Foss, A.J.E.; Almeida, D.; Cheung, C.M.G.; Ogura, Y.; de Cock, E.; Empeslidis, T. To Treat or Not to Treat? Resolving the Question of Subretinal and Intraretinal Fluid in Age-Related Macular Degeneration: A Narrative Review. *Ophthalmol. Ther.* **2025**, *14*, 489–514. [CrossRef] [PubMed]
27. Spooner, K.L.; Fraser-Bell, S.; Mehta, H.; Hong, T.; Broadhead, G.; Wong, J.G.; Chang, A.A. Lost to Follow-Up in Neovascular Age-Related Macular Degeneration: A Systematic Review of Global Trends, Risk Factors, and Clinical Consequences. *Ophthalmologica* **2026**, *249*, 79–102. [CrossRef] [PubMed]

Disclaimer/Publisher's Note: The statements, opinions and data contained in all publications are solely those of the individual author(s) and contributor(s) and not of MDPI and/or the editor(s). MDPI and/or the editor(s) disclaim responsibility for any injury to people or property resulting from any ideas, methods, instructions or products referred to in the content.